

# A link between measured neutron star masses and lattice QCD data

Ignazio Bombaci<sup>1\*</sup> and Domenico Logoteta<sup>2</sup>

<sup>1</sup>*Dipartimento di Fisica ‘Enrico Fermi’, Università di Pisa, and INFN Sezione di Pisa, Largo Bruno Pontecorvo 3, I-56127 Pisa, Italy*

<sup>2</sup>*Centro de Física Computacional, Department of Physics, University of Coimbra, 3004-516 Coimbra, Portugal*

Accepted 2013 May 16. Received 2013 May 14; in original form 2013 January 29

## ABSTRACT

We study the hadron–quark phase transition in neutron star matter and the structural properties of hybrid stars using an equation of state (EOS) for the quark phase derived with the field correlator method (FCM). We make use of the measured neutron star masses, and particularly the mass of PSR J1614–2230, to constrain the values of the gluon condensate  $G_2$  which is one of the EOS parameter within the FCM. We find that the values of  $G_2$  extracted from the mass measurement of PSR J1614–2230 are fully consistent with the values of the same quantity derived, within the FCM, from recent lattice quantum chromodynamics (QCD) calculations of the deconfinement transition temperature at zero baryon chemical potential. The FCM thus provides a powerful tool to link numerical calculations of QCD on a space–time lattice with neutron stars physics.

**Key words:** dense matter – equation of state – stars: neutron

## 1 INTRODUCTION

Neutron stars, the compact remnants of supernova explosions, are unique natural laboratories to explore the phase diagram of quantum chromodynamics (QCD) in the low-temperature  $T$  and high-baryon-chemical-potential  $\mu_b$  region (Weber 2005; Alford et al. 2008). In this regime non-perturbative aspects of QCD are expected to play a crucial role, and a transition to a phase with deconfined quarks and gluons is expected to occur and to influence a number of interesting astrophysical phenomena (Perez-Garcia et al. 2010; Sotani et al. 2011; Berezhiani et al. 2003; Lugones & Bombaci 2005; Bombaci et al. 2011).

Recent high-precision numerical calculations of QCD on a space–time lattice at  $\mu_b = 0$  (i.e. zero baryon density) have shown that at high temperature and for physical values of the quark masses, the transition to quark gluon plasma is a crossover (Aoki et al. 2006) rather than a real phase transition.

Unfortunately, present lattice QCD calculations at finite baryon chemical potential are unrealizable by all presently known lattice methods (see e.g. Lombardo (2008)). Thus, to explore the QCD phase diagram at low  $T$  and high  $\mu_b$ , it is necessary to invoke some approximations in QCD or to apply some QCD effective model.

Along these lines, different models of the equation

of state (EOS) of quark matter, as the bag model (Farhi & Jaffe 1984) or the Nambu–Jona-Lasinio (NJL) model (Nambu & Jona-Lasinio 1961; Buballa 2005), have been intensively used by many authors to calculate the structure of strange stars (Witten 1984; Alcock et al. 1986; Haensel et al. 1986), or the structure of the so called hybrid stars, *i.e.* neutron stars with a quark matter core (see e.g. Klähn et al. (2007); Lenzi & Lugones (2012)). These EOS models are expected to be reasonable at very large density, but they crumbles in the density region where quarks clusterize to form hadrons, *i.e.* in the region where the deconfinement phase transition takes place. In addition, the bag model and the NJL model, as other QCD effective models, can not make predictions in the high  $T$  and zero  $\mu_b$  region, and thus cannot be tested using present lattice QCD calculations.

A promising approach to describe the EOS of the quark gluon phase is the so called Polyakov loop extended NJL model (Meisinger & Ogilvie 1996; Fukushima 2004; Ratti et al. 2006; Blaschke et al. 2008; Contrera et al. 2008; Blaschke et al. 2010; Dexheimer & Schramm 2010), which combines the two main nonperturbative aspects of low energy QCD: confinement and spontaneous chiral symmetry breaking.

Recently the deconfinement phase transition has been described using an EOS of quark gluon plasma derived within the field correlator method (FCM) (Dosch 1987; Di Giacomo et al. 2002) extended to finite baryon chemical potential (Simonov & Trusov 2007; Simonov 2005, 2008;

\* E-mail: bombaci@df.unipi.it

Nefediev et al. 2009). The FCM is a nonperturbative approach to QCD which includes from first principles the dynamics of confinement. The model is parametrized in terms of the gluon condensate  $G_2$  and the large distance static  $Q\bar{Q}$  potential  $V_1$ . These two parameters control the EOS of the deconfined phase at fixed quark masses and temperature. The main constructive characteristic of the FCM is the possibility of describing the whole QCD phase diagram as it can span from high temperature and low baryon chemical potential, to low  $T$  and high  $\mu_b$  limit.

A very interesting feature of the FCM is that the value of the gluon condensate can be obtained from lattice QCD calculations of the deconfinement transition temperature  $T_c$ , at zero baryon chemical potential. Thus, we have an efficacious tool to directly link lattice QCD simulations and neutron star physics.

To explore this link is the main purpose of this work. In particular, we will investigate the possibility for the occurrence of the quark deconfinement transition in neutron stars and the possibility of having stable hybrid star configurations using the FCM for the quark phase EOS and a relativistic mean field model (Glendenning & Moszkowski 1991) for the EOS of the hadronic phase.

## 2 EOS OF THE QUARK PHASE

The quark matter EOS we used in this work is based on the FCM (Dosch 1987; Di Giacomo et al. 2002). Recently, this method has been extended to the case of non-zero baryon density (Simonov & Trusov 2007; Simonov 2005, 2008; Nefediev et al. 2009) making possible its application to neutron star matter.

The main advantage of the FCM is a natural explanation and treatment of the dynamics of confinement in terms of colour electric  $D^E(x)$ ,  $D_1^E(x)$  and colour magnetic  $D^H(x)$ ,  $D_1^H(x)$  Gaussian correlators (Di Giacomo et al. 2002).  $D^E$  contributes to the standard string tension  $\sigma^E$  through (Simonov & Trusov 2007):

$$\sigma^E = \frac{1}{2} \int D^E(x) d^2x. \quad (1)$$

The string tension  $\sigma^E$  vanishes as  $D^E$  goes to zero at  $T \geq T_c$ , and this leads to deconfinement. The correlators have been calculated on the lattice (D'Elia et al. 2003) and also analytically (Simonov 2006).

Within the FCM the quark pressure  $P_q$ , for a single flavour, reads (Simonov & Trusov 2007)

$$P_q/T^4 = \frac{1}{\pi^2} [\phi_\nu(\frac{\mu_q - V_1/2}{T}) + \phi_\nu(-\frac{\mu_q + V_1/2}{T})] \quad (2)$$

where

$$\phi_\nu(a) = \int_0^\infty du \frac{u^4}{\sqrt{u^2 + \nu^2}} \frac{1}{(\exp[\sqrt{u^2 + \nu^2} - a] + 1)}, \quad (3)$$

$\nu = m_q/T$  and  $V_1$  is the large distance static  $Q\bar{Q}$  potential:

$$V_1(T) = \int_0^{1/T} d\tau (1 - \tau T) \int_0^\infty d\chi \chi D_1^E(\sqrt{\chi^2 + \tau^2}). \quad (4)$$

The non-perturbative contribution to  $D_1^E(x)$  is parametrized as (Di Giacomo et al. 2002)

$$D_1^E(x) = D_1^E(0) \exp(-|x|/\lambda) \quad (5)$$

where  $\lambda$  is the vacuum correlation length. Following Simonov & Trusov (2007), we use the value  $\lambda = 0.34$  fm which has been determined in lattice QCD calculations (D'Elia et al. 1997).

In this formalism,  $V_1$  in equation(4) is independent of the chemical potential (and so on the density). This feature is partially supported by lattice simulations at small chemical potential (Simonov & Trusov 2007; Doring et al. 2006). In this work, the value of  $V_1$  at  $T = 0$  has been considered as a model parameter.

The gluon contribution to the pressure is (Nefediev et al. 2009)

$$P_g/T^4 = \frac{8}{3\pi^2} \int_0^\infty d\chi \chi^3 \frac{1}{\exp(\chi + \frac{9V_1}{8T}) - 1}. \quad (6)$$

In summary the total pressure of the quark phase is given by

$$P_{qq} = P_g + \sum_{u,d,s} P_q - \frac{9}{64} G_2. \quad (7)$$

The last term in equation(7) represents the vacuum energy difference between the quark and hadronic phases, in the case of three flavour ( $u$ ,  $d$ ,  $s$ ) quark matter (Simonov & Trusov 2007), and  $G_2$  is the gluon condensate. The latter quantity has been determined, with large uncertainty, using QCD sum rules (Shifman et al. 1979)  $G_2 = (0.012 \pm 0.006)$  GeV<sup>4</sup>. In this work, the value of  $G_2$  has been considered as a model parameter. We used the following values of the current-quark masses:  $m_u = m_d = 5$  MeV and  $m_s = 150$  MeV. In summary, the quark matter EOS has two parameters:  $G_2$  and  $V_1 = V_1(T = 0)$ .

## 3 NEUTRON STAR STRUCTURE

In this section, we show the results of our calculations of hybrid stars structure. To this purpose, we integrate the well-known Tolman, Oppenheimer and Volkov relativistic hydrostatic equilibrium equations to get various stellar properties for a fixed EOS. For the hadronic phase, we consider  $\beta$ -stable nuclear matter, and we make use of a non-linear relativistic mean field model in the parametrization GM1 given by Glendenning & Moszkowski (1991). The GM1 model can be considered a representative realistic nuclear EOS in the sense that it fits the empirical saturation properties of nuclear matter, does not violate causality at high density and is compatible with the present measured neutron star masses. All the results presented in the following have been obtained using the Gibbs construction (Glendenning 1992) to model the hadron-quark phase transition.

In Fig. 1 we report the stellar gravitational mass  $M$  (in unit of the solar mass  $M_\odot = 1.99 \times 10^{33}$  g) versus the central baryon number density  $\rho_c$  (left-hand panel) and the mass versus radius  $R$  (right-hand panel) in the case of pure nucleonic stars (continuous line) and of hybrid stars for different  $G_2$  and taking  $V_1 = 0.01$  GeV. We obtain stable hybrid star configurations for all the considered values of the gluon condensate, with maximum masses ranging from  $M_{max} = 1.44 M_\odot$  (case with  $G_2 = 0.006$  GeV<sup>4</sup>) to  $M_{max} = 2.05 M_\odot$  ( $G_2 = 0.0016$  GeV<sup>4</sup>). Note that the hybrid

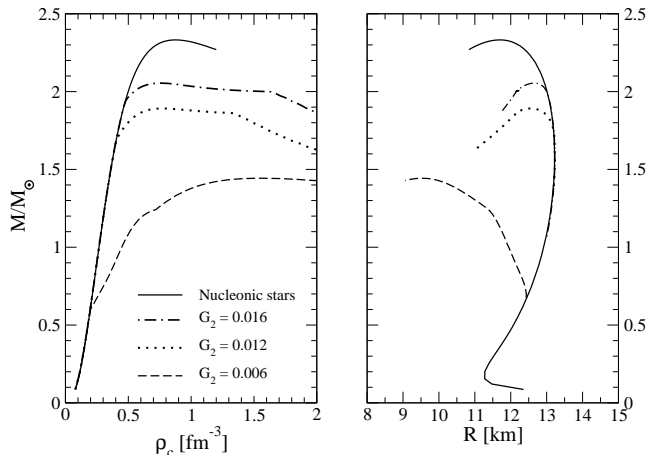


**Figure 1.** Stellar gravitational mass  $M$  versus central baryon number density  $\rho_c$  (left-hand panel) and versus stellar radius  $R$  (right-hand panel) for hybrid stars for several values of the gluon condensate  $G_2$  (reported in  $\text{GeV}^4$  units) and for  $V_1 = 0.01 \text{ GeV}$ . The continuous line in both panels refers to the pure nucleonic stars, i.e. compact stars with no quark matter content.

**Table 1.** Properties of the maximum mass configuration for hybrid stars as a function of the gluon condensate  $G_2$ .

$G_2$ ( $\text{GeV}^4$ )	$M_{max}$ ( $M_\odot$ )	$\rho_c^{Hyb}$ ( $\text{fm}^{-3}$ )	$R$ (km)
0.006	1.44	1.55	9.54
0.012	1.89	0.77	12.55
0.016	2.05	0.75	12.66

The results are relative to the case  $V_1 = 0.01 \text{ GeV}$ . The maximum mass configuration for the pure nucleonic star sequence is:  $M_{max} = 2.33 M_\odot$ ,  $\rho_c^{NS} = 0.87 \text{ fm}^{-3}$  and  $R = 11.70 \text{ km}$ .

star branch of the stellar equilibrium configurations shrinks as  $G_2$  is increased. This behaviour is different with respect to the one found by Baldo et al. (2008), where the stability window of hybrid star configurations was restricted within the range  $0.006 \text{ GeV}^4 < G_2 < 0.007 \text{ GeV}^4$ .

The properties of the maximum mass configuration for hybrid star sequences varying  $G_2$  are summarized in table 1.

In Fig. 2, we plot the quark–hadron phase transition boundaries in  $\beta$ -stable nuclear matter as a function of  $G_2$  and with  $V_1 = 0.01 \text{ GeV}$ . The onset of the deconfinement transition (i.e. the onset of the quark–hadron mixed phase) occurs at the baryon number density  $\rho_1$ , and the pure quark phase begins at  $\rho_2$ . Also, shown is the central baryon number density  $\rho_c^{Hyb}$  of the maximum mass hybrid star (dot–dashed line). Stable hybrid star configurations have central densities  $\rho_c$  located in the region of the  $\rho$ – $G_2$  plane between the lower continuous line and the dot–dashed line, i.e.  $\rho_1 < \rho_c \leq \rho_c^{Hyb}$ . Note that  $\rho_c^{Hyb} > \rho_2$  when the gluon condensate is in the range  $0.006 \text{ GeV}^4 < G_2 \leq 0.0077 \text{ GeV}^4$ . For these  $G_2$  values all hybrid stars with a central density in the range  $\rho_2 < \rho_c \leq \rho_c^{Hyb}$  possess a pure quark matter core. Finally the horizontal dashed line represents the value  $\rho_c^{NS}$  of the central baryon number density of the maximum mass pure nucleonic star.

In Fig. 3 we draw the maximum mass  $M_{max}$  for hybrid stars (continuous line) and the mass  $M_1 = M(\rho_1)$  (dashed

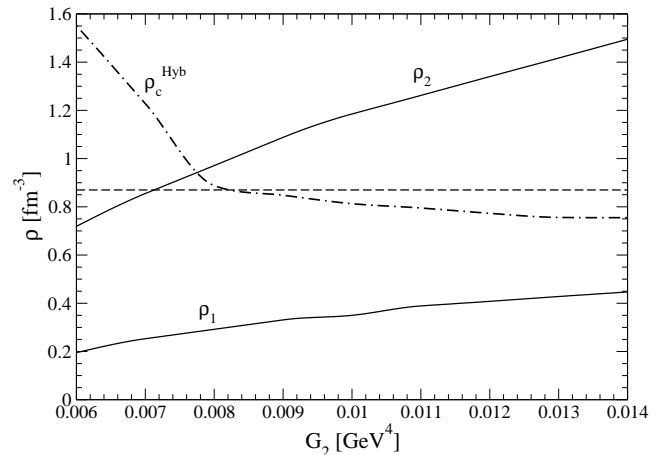


**Figure 2.** Quark–hadron phase transition boundaries in  $\beta$ -stable nuclear matter as a function of the gluon condensate  $G_2$  and for  $V_1 = 0.01 \text{ GeV}$ . The onset of quark–hadron mixed phase occurs at the baryon number density  $\rho_1$ , and the pure quark phase begins at  $\rho_2$ . Also shown is the central baryon number density  $\rho_c^{Hyb}$  of the maximum mass hybrid star. The horizontal dashed line represents the value  $\rho_c^{NS}$  of the central baryon number density of the maximum mass pure nucleonic star.

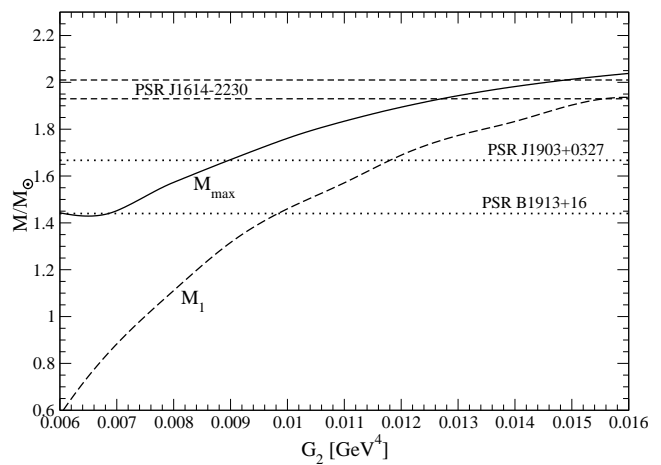


**Figure 3.** Gravitational maximum mass for hybrid stars (continuous line) and gravitational mass  $M_1$  (dashed line) of the star with central baryon number density  $\rho_1$  corresponding to the onset of mixed quark–hadron phase as a function of the gluon condensate  $G_2$  and for  $V_1 = 0.01 \text{ GeV}$ .

line) of the star with central baryon number density  $\rho_1$  corresponding to the onset of the mixed phase. These two quantities are plotted as a function of the gluon condensate  $G_2$  and taking  $V_1 = 0.01 \text{ GeV}$ . Stable hybrid star configurations correspond to the region of the  $M$ – $G_2$  plane between the continuous and the dashed line. Stellar configurations in the region below the dashed line  $M_1$  do not possess any deconfined quark matter in their centre (pure nucleonic stars).

To compare our results with measured neutron star masses, we report in the same Fig. 3, the values of the masses of the following pulsars: PSR B1913+16

with  $M = 1.4398 \pm 0.0002 M_\odot$  (Hulse & Taylor 1975; Weisberg et al. 2010), PSR J1903+0327 with  $M = 1.667 \pm 0.021 M_\odot$  (Freire et al. 2011) and PSR J1614–2230 with  $M = 1.97 \pm 0.04 M_\odot$  (Demorest et al. 2010).

The mass of PSR J1614–2230 gives the strongest constraint on the possible value of the gluon condensate. In fact, using the lower bound of the measured mass of PSR J1614–2230, we get  $G_2 \geq 0.0129 \text{ GeV}^4$ . Thus, for values of the gluon condensate in the range  $0.0129 \text{ GeV}^4 \leq G_2 \leq G_2^* \simeq 0.018 \text{ GeV}^4$ , PSR J1614–2230 is a hybrid star, whereas PSR B1913+16 and PSR J1903+0327 are pure nucleonic stars. In the above specified range for the gluon condensate,  $G_2^*$  is defined by the condition  $M_1(G_2^*) = 2.01 M_\odot$ , the upper bound of the measured mass of PSR J1614–2230. Thus for  $G_2 > G_2^*$ , PSR J1614–2230 is a pure nucleonic star.

To explore the influence of the large distance static  $Q\bar{Q}$  potential on the stellar properties, we have considered a quark phase EOS with  $V_1 = 0.10 \text{ GeV}$ . Once again we get stable hybrid star configurations for all the considered values of  $G_2$ , with maximum masses ranging from  $M_{max} = 2.00 M_\odot$  (case with  $G_2 = 0.006 \text{ GeV}^4$ ) to  $M_{max} = 2.25 M_\odot$  ( $G_2 = 0.0016 \text{ GeV}^4$ ). Thus an increase of the value of  $V_1$  reduces the extension of the hybrid star branch, shifts it to larger densities and produces hybrid stars with a larger maximum mass. In this case we found that the calculated  $M_{max}$  is compatible with the lower bound of the measured mass of PSR J1614–2230 for all the considered values of the gluon condensate (i.e.  $G_2 \geq 0.006 \text{ GeV}^4$ ).

We also considered stellar models with  $V_1 = 0.50 \text{ GeV}$  and  $V_1 = 0.85 \text{ GeV}$ . In these two cases no phase transition occurs in neutron stars (i.e.  $\rho_1 > \rho_c^{NS}$  the central density of the maximum mass pure nucleonic star), thus in this case PSR J1614–2230 would be a pure nucleonic star.

#### 4 LATTICE QCD CALCULATIONS AND MEASURED NEUTRON STAR MASSES

Within the FCM, the deconfinement transition temperature  $T_c$  at  $\mu_b = 0$  reads (Simonov & Trusov 2007)

$$T_c = \frac{a_0}{2} G_2^{1/4} \left( 1 + \sqrt{1 + \frac{V_1(T_c)}{2a_0 G_2^{1/4}}} \right), \quad (8)$$

with  $a_0 = (3\pi^2/768)^{1/4}$  in the case of three flavours. In their analysis, Simonov & Trusov (2007) assume  $V_1(T_c) = 0.5 \text{ GeV}$ , thus,  $T_c$  in equation (8) is a simple function of  $G_2$ , and is represented in Fig. 4 by the curve labelled  $V_1(T_c) = 0.5 \text{ GeV}$ . This result can hence be compared with lattice QCD calculations of  $T_c$  giving the possibility of extracting the range of values for the gluon condensate compatible with lattice results. This comparison has been done by Simonov & Trusov (2007), and it is done in this work in Fig. 4, where we consider recent lattice QCD calculations of  $T_c$  (Borsanyi et al. 2010; Bazavov et al. 2012). Details to the specific lattice QCD calculations are given in the caption to Fig. 4. As one can see, the comparison with lattice QCD calculations of  $T_c$  restricts the gluon condensate in a rather narrow range  $G_2 = 0.0025\text{--}0.0050 \text{ GeV}^4$ .

Next, to verify if these values of  $G_2$  are compatible with those extracted in Section 3 from hybrid star calculations

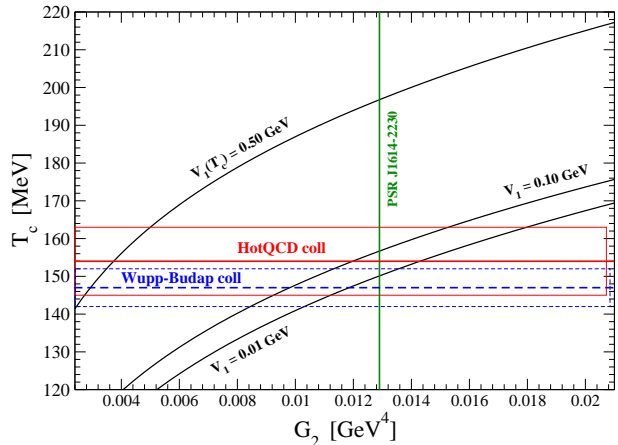


**Figure 4.** (Deconfinement transition temperature  $T_c$  at  $\mu_b = 0$ . The curve labeled with  $V_1(T_c) = 0.5 \text{ GeV}$  reproduces the FCM results of Simonov & Trusov (2007) for a fixed value  $V_1(T_c) = 0.5 \text{ GeV}$  of the large distance static  $Q\bar{Q}$  potential. The curve labelled with  $V_1 = 0.01 \text{ GeV}$  ( $V_1 = 0.10 \text{ GeV}$ ) corresponds to the transition temperature at  $\mu_b = 0$  obtained solving numerically equations (8) and (9) for the case  $V_1(0) = 0.01 \text{ GeV}$  [ $V_1(0) = 0.10 \text{ GeV}$ ]. The horizontal heavy and thin lines represent, respectively, the central value and the error estimate of lattice QCD calculations. In particular, the red continuous lines refer to the calculations (Bazavov et al. 2012) of the Hot QCD collaboration  $T_c = (154 \pm 9) \text{ MeV}$ ; the blue short dashed lines refer to the calculations (Borsanyi et al. 2010) of the Wuppertal–Budapest collaboration  $T_c = (147 \pm 5) \text{ MeV}$ . Finally, the vertical green line represents the lower limit for  $G_2$  which is compatible with the lower bound of the measured mass of PSR J1614–2230 for the case  $V_1(0) = 0.01 \text{ GeV}$ .

and measured neutron star masses, we need to relate the parameter  $V_1 \equiv V_1(0)$ , entering in the zero temperature EOS of the quark phase, with  $V_1(T_c)$  in equation (8). To this end, one can integrate equation (4) using the non-perturbative contribution of equation (5) to the colour electric correlator  $D_1^E(x)$  and assuming that the normalization factor  $D_1^E(0)$  does not depend on temperature. The latter assumption is supported, up to temperatures very near to  $T_c$ , by lattice calculations (D’Elia et al. 2003). Therefore, one gets

$$V_1(T) = V_1(0) \left\{ 1 - \frac{3\lambda T}{2\hbar c} + \frac{1}{2} \left( 1 + 3\frac{\lambda T}{\hbar c} \right) e^{-\frac{\hbar c}{\lambda T}} \right\}. \quad (9)$$

Thus,  $V_1(T_c) = 0.5 \text{ GeV}$  (Simonov & Trusov 2007) corresponds to  $V_1(0) = 0.85 \text{ GeV}$  to be used in the  $T = 0$  EOS of the quark phase. In this case, as we found in Section 3, no phase transition occurs in neutron stars (i.e.  $\rho_1 > \rho_c^{NS}$ ) for all the considered values of  $G_2$ . Thus, for these values of the EOS parameters PSR J1614–2230 would be a pure nucleonic star.

We can also evaluate the FCM transition temperature at  $\mu_b = 0$  corresponding to the case  $V_1(0) = 0.01 \text{ GeV}$  used in Section 3 for hybrid star calculations with the  $T = 0$  FCM EOS. To this purpose, we solve numerically equations (8) and (9), and we obtain the results represented in Fig. 4 by the curve labelled  $V_1 = 0.01 \text{ GeV}$ . The comparison of these results with lattice QCD calculations (Borsanyi et al. 2010; Bazavov et al. 2012) of  $T_c$  restricts the gluon condensate in the range  $G_2 = 0.0103\text{--}0.0180 \text{ GeV}^4$ . Coming now to the astrophysical constraints on the gluon condensate, the vertical

green line in Fig. 4 represents the lower limit for  $G_2$  which is compatible, in the case  $V_1(0) = 0.01$  GeV, with the lower bound of the measured mass of PSR J1614–2230 (see Section 3).

A similar analysis can be done for the case  $V_1(0) = 0.10$  GeV. Now the comparison between the FCM transition temperature at  $\mu_b = 0$  (curve labelled  $V_1 = 0.10$  GeV in Fig. 4) and lattice QCD calculations of the same quantity gives  $G_2 = 0.0085\text{--}0.0153$  GeV<sup>4</sup>, whereas one gets  $G_2 \geq 0.006$  GeV<sup>4</sup> from the lower bound of the measured mass of PSR J1614–2230.

## 5 CONCLUSIONS

In this Letter, we have studied the hadron–quark deconfinement transition in  $\beta$ -stable nuclear matter and the structural properties of hybrid stars using an EOS for the quark phase derived from the FCM extended to finite baryon chemical potential. We obtained stable hybrid star configurations for all the values of the gluon condensate fulfilling the condition  $\rho_1(G_2) < \rho_c^{NS}(G_2)$ , i.e. the deconfinement transition can occur in pure nucleonic stars.

We have established that the values of the gluon condensate extracted within the FCM from lattice QCD calculations of the deconfinement transition temperature at  $\mu_b = 0$  are fully consistent with the value of the same quantity derived by the mass measurement of PSR J1614–2230. The FCM thus provides a powerful tool to link numerical calculations of QCD on a space–time lattice with neutron stars physics.

## ACKNOWLEDGEMENTS

It is a pleasure to thank Claudio Bonati for very useful discussions.

## REFERENCES

- Alcock C., Farhi E., Olinto A., 1986, *ApJ*, 310, 261  
 Alford M.G., Schmitt A., Rajagopal K., Schafer T., 2008, *Rev. Mod. Phys.*, 80, 1455  
 Aoki Y., Endrodi G., Fodor Z., Katz S.D., Szabó K.K., 2006, *Nat*, 443, 675  
 Baldo M., Burgio G.F., Castorina P., Plumari S., Zappalà D., 2008, *Phys. Rev. D*, 78, 063009  
 Bazavov A., et al., 2012, *Phys. Rev. D*, 85, 054503  
 Berezhiani Z., Bombaci I., Drago A., Frontera F., Lavagno A., 2003, *ApJ*, 586, 1250  
 Blaschke D., Buballa M., Radzhabov A. E., Volkov M. K., 2008, *Phys. At. Nucl.*, 71, 1981  
 Blaschke D., Berdermann J., Lastowiecki R., 2010, *Prog. Theor. Phys. Suppl.*, 186, 81  
 Bombaci I., Logoteta D., Providência C., Vidaña, I., 2011, *A&A*, 528, A71  
 Borsanyi S., et al, 2010, *J. High Energy Phys.*, 09, 073  
 Buballa M., 2005, *Phys. Rep.*, 407, 205  
 Contrera G. A., Gómez Dumm D., Scoccola N. N., 2008, *Phys. Lett. B* 661, 113  
 D’Elia M., Di Giacomo A., Meggiolaro E., 1997, *Phys. Lett. B* 408, 315  
 D’Elia M., Di Giacomo A., Meggiolaro E., 2003, *Phys. Rev. D*, 67, 114504  
 Demorest P., Pennucci T., Ransom S., Roberts M., Hessels J., 2010, *Nature*, 467, 1081  
 Dexheimer V. A., Schramm S., 2010, *Nucl. Phys. B*, 199, 319  
 Di Giacomo A., Dosch H.G., Shevchenko V.I., Simonov Y.A., 2002, *Phys. Rep.*, 372, 319  
 Doring M., Ejiri S., Kaczmarek O., Karsch F., Laermann E., 2006, *Eur. Phys. J.*, C46, 179  
 Dosch H.G., 1987, *Phys. Lett. B*, 190, 177; Dosch H.G., Simonov Yu., 1988, *Phys. Lett. B*, 205, 339; Simonov Yu., 1988, *Nucl. Phys. B*, 307, 512  
 Farhi E., Jaffe R.L., 1984, *Phys. Rev. D*, 30, 272  
 Freire P.C.C., et al., 2011, *MNRAS*, 412, 2763  
 Fukushima K., 2004, *Phys. Lett. B*, 591, 277  
 Glendenning N.K., Moszkowski S., 1991, *Phys. Rev. Lett.*, 67, 2414  
 Glendenning N.K., 1992, *Phys. Rev. D*, 46, 1274  
 Haensel P., Zdunik J.L., Schaefer R., 1986, *A&A* 160, 121  
 Hulse R.A., Taylor J.H., 1975, *ApJ*, 195, L51  
 Klähn T. et al., 2007, *Phys. Lett. B* 654, 170  
 Lenzi C. H., Lugones G., 2012, *ApJ*, 759, 57  
 Lombardo M.P., 2008, *J. Phys. G*, 35, 104019  
 Lugones G., Bombaci I., 2005, *Phys. Rev. D*, 72, 065021  
 Meisinger P. N., Ogilvie M. C., 1996, *Phys. Lett. B* 379, 163.  
 Nambu Y., Jona-Lasinio G., 1961, *Phys. Rev.* 122, 345.  
 Nefediev A.V., Simonov Yu.A., Trusov A.M., 2009, *Int. J. Mod. Phys. E*, 18, 549.  
 Perez-Garcia M.A., Silk J., Stone J.R., 2010, *Phys. Rev. Lett.*, 105, 141101  
 Ratti C., Thaler M. A., Weise W., 2006, *Phys. Rev. D*, 73, 014019  
 Shifman M.A., Vainshtein A.I., Zakharov, V.I., 1979, *Nucl. Phys. B*147, 385; *Nucl. Phys. B*147, 448.  
 Simonov Yu.A., Trusov, M.A., 2007, *JETP Lett.* 85, 598; Simonov Yu.A., Trusov, M.A., 2007, *Phys. Lett. B*, 650, 36 (ST07)  
 Simonov Yu.A., 2005, *Phys. Lett. B*, 619, 293  
 Simonov Yu.A., 2006, *Phys. At. Nucl.*, 69, 528  
 Simonov Yu.A., 2008, *Ann. Phys.*, 323, 783  
 Sotani H., Yasutake N., Maruyama T., Tatsumi T., 2011, *Phys. Rev. D*, 83, 024014  
 Weber F., 2005, *Prog. Part. Nucl. Phys.*, 54, 193  
 Weisberg J.M., Nice D.J., Taylor J.H., 2010, *ApJ*, 722, 1030  
 Witten E., 1984, *Phys. Rev. D*, 30, 272